

Are We Truly Forgetting? A Critical Re-examination of Machine Unlearning Evaluation Protocols

Yongwoo Kim^{*1} Sungmin Cha^{*2} Donghyun Kim^{†1}

¹Korea University ²New York University

Abstract

Machine unlearning is a process to remove specific data points from a trained model while maintaining the performance on retain data, addressing privacy or legal requirements. Despite its importance, existing unlearning evaluations tend to focus on logit-based metrics (i.e., accuracy) under small-scale scenarios. We observe that this could lead to a false sense of security in unlearning approaches under real-world scenarios. In this paper, we conduct a new comprehensive evaluation that employs representation-based evaluations of the unlearned model under large-scale scenarios to verify whether the unlearning approaches genuinely eliminate the targeted forget data from the model’s representation perspective. Our analysis reveals that current state-of-the-art unlearning approaches either completely degrade the representational quality of the unlearned model or merely modify the classifier (i.e., the last layer), thereby achieving superior logit-based evaluation metrics while maintaining significant representational similarity to the original model. Furthermore, we introduce a novel unlearning evaluation setup from a transfer learning perspective, in which the forget set classes exhibit semantic similarity to downstream task classes, necessitating that feature representations diverge significantly from those of the original model. Our comprehensive benchmark not only addresses a critical gap between theoretical machine unlearning and practical scenarios, but also establishes a foundation to inspire future research directions in developing genuinely effective unlearning methodologies.

1. Introduction

Neural networks have driven transformative advancements across a multitude of domains, such as image classification [10, 17, 25]. A key contributor to this progress has been the substantial enhancement of the model capability, facilitated by the training of sophisticated models on vast

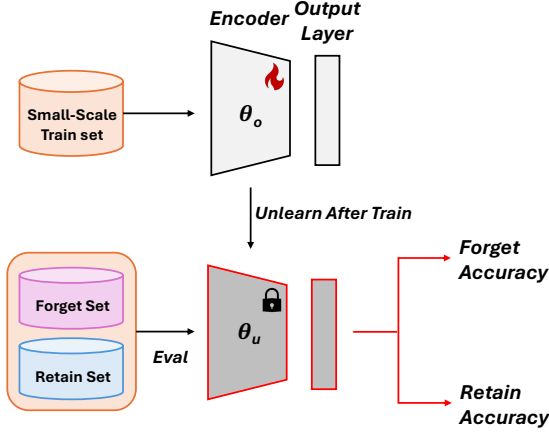
datasets [1]. However, these successes have also raised significant privacy concerns in these datasets, particularly related to the unchecked use of sensitive data [4]. As privacy rights, including the ‘right to be forgotten’ (e.g., the GDPR legislation [3, 27]), have gained increasing recognition, the need for effective solutions has become urgent. As a result, this has led to the emergence of machine unlearning as a critical area of research [28].

The primary objective of machine unlearning is to effectively eliminate the influence of specific data from a pre-trained model while preserving the knowledge derived from other data [28]. The most straightforward approach, known as *exact unlearning*, involves retraining the model from scratch using a refined dataset [26] (hereafter referred to as the “*retrained model*”). While this approach is regarded as the gold standard because it guarantees complete elimination of any influence from data designated for removal, it incurs significant computational expenses due to the necessity of retraining models on refined datasets whenever unlearning is required. To overcome these limitations, several *approximate unlearning* algorithms have been proposed, offering more efficient alternatives while striving to maintain the goal of machine unlearning [16]. In image classification tasks, approximate unlearning algorithms are typically evaluated based on their ability to produce models that achieve classification accuracy similar to that of the exact unlearning on the given dataset (e.g., retain and forget sets) [28], as illustrated on the left side of Fig. 1. Following this evaluation method, several methods have induced unlearning through techniques such as using random labeling [14], gradient ascent [32] and metric learning [2], while mitigating the over-forgetting by incorporating additional regularization terms [2, 6, 12, 23].

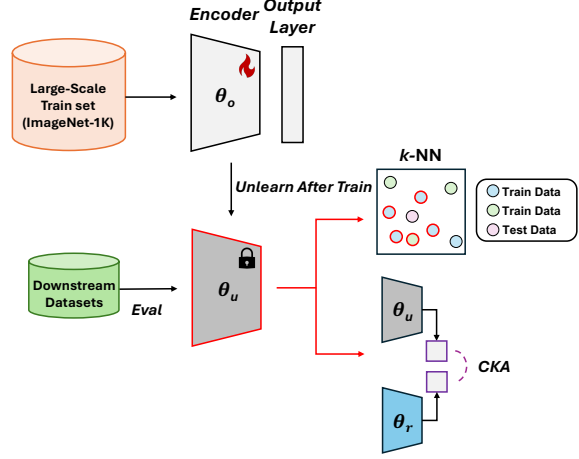
Despite recent advancements, current evaluations of approximate unlearning research remain confined to logit-based evaluation (e.g., classification accuracy) on small-scale unlearning tasks and datasets, such as unlearning a limited number of classes for models trained on CIFAR-10 and CIFAR-100 [22], as shown in Fig. 1a. Such narrow evaluation scopes raise significant concerns about the scalability of these methods to larger datasets and real-

^{*}First authors

[†]Corresponding author



(a) Traditional evaluation framework.



(b) Our proposed evaluation framework.

Figure 1. A comparison of (a) the traditional evaluation framework and (b) our proposed evaluation framework. Note that θ_u and θ_r refer to the unlearned model and the model trained on the retain set, respectively. Traditional unlearning evaluation methods primarily focus on analyzing the unlearned model’s output logits to assess the effectiveness of unlearning under small-scale scenarios such as CIFAR-10. In contrast, our framework introduces additional evaluation factors by examining the unlearned model’s feature representations in terms of transferability and similarity under the large-scale unlearning scenario, such as using ImageNet-1k.

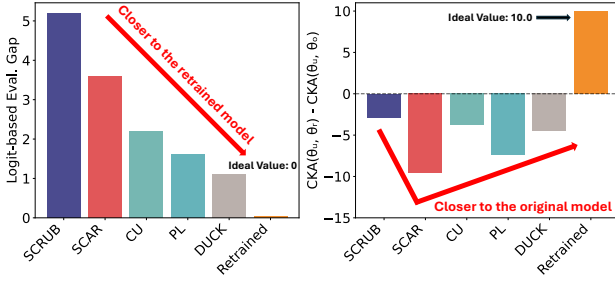


Figure 2. Performance comparison between logit-based (left) and representation-based evaluation (right) reveals contrasting findings. In the left figure, logit-based metrics suggest that the unlearned model (θ_u) performs similarly to the retrained model (θ_r), implying seemingly successful unlearning. However, the right figure, which presents our proposed representation-based evaluation, shows a different trend. Negative values in the right figure indicate that the unlearned model remains closer to the original model (θ_o) than to the retrained model (θ_r), revealing that none of the unlearning approaches achieve greater similarity to θ_r than to θ_o .

world unlearning scenarios. Privacy considerations assume heightened significance in larger model architectures (e.g., foundation models), as these systems are trained on extensive datasets frequently sourced from web-crawled images, subsequently employed across diverse downstream applications. This limitation overlooks the broader implications of unlearning algorithms on the model’s foundational component (i.e., encoder), potentially leading to incomplete or misleading assessments of its effectiveness.

In this paper, we propose a comprehensive new evaluation framework that addresses the limitations of existing small-scale, logit-based evaluations by incorporating assessments of unlearned models (θ_u) from the perspective

of feature representations in large-scale settings. As illustrated in Fig. 1b, our framework evaluates the representations of unlearned models using Centered Kernel Alignment (CKA) [20] to compare the feature representations of the unlearned models with those of a model trained only on the retain set (θ_r). Additionally, we apply k -Nearest Neighbors (k -NN) analysis on the feature space across various downstream datasets to assess the quality of feature representations. Through these evaluation methods, we re-evaluate multiple state-of-the-art unlearning algorithms in the large-scale unlearning scenario. Fig. 2 illustrates key findings from experiments on unlearning 100 random classes in ImageNet-1k using ResNet-50: while logit-based evaluation (e.g., classification accuracy) demonstrates successful unlearning by showing a decreasing gap between the unlearned models (θ_u) and the retrained model (θ_r) (Fig. 2, left), a representation-based evaluation using CKA reveals a critical limitation (Fig. 2, right). In an ideal scenario, where unlearning is truly effective, the unlearned model should be indistinguishable from the retrained model, with the ideal value being 10. However, as shown in Fig. 2 (right), all unlearned models exhibit greater similarity to the original model than to the retrained model. This highlights a fundamental issue: existing unlearning methods fail to sufficiently erase learned information at the representation level. This reinforces the need for representation-based evaluation to rigorously assess whether unlearning truly eliminates the influence of the targeted data. Furthermore, random class forgetting has been widely adopted as a standard evaluation scenario in unlearning studies [2, 6, 12, 23]. However, we highlight a critical limitation of this approach: the forgetting process may be inadequately assessed, as similar represen-

tational knowledge can persist across multiple alternative classes, making it difficult to verify whether the targeted data has been truly unlearned. To address this issue, we propose a novel unlearning evaluation paradigm, *Top Class-wise Forgetting*, in which the classes selected for unlearning are semantically similar to those in downstream tasks. This setup requires a substantial divergence of feature representations from the original model, offering a more rigorous assessment of unlearning algorithm’s effectiveness. We then evaluate existing unlearning methods using both logit-based and representation-based metrics across diverse downstream datasets. In summary, the core contributions are summarized as follows:

- We explore new evaluation metrics for unlearning from a representational perspective under large-scale settings, demonstrating that existing unlearning models exhibit limited effectiveness or fail to genuinely eliminate targeted data.
- We propose a new evaluation setting, Top Class-wise Forgetting, which overcomes the limitations of random class forgetting and enables a more comprehensive assessment of unlearning through diverse downstream tasks from a transfer learning perspective.
- Our experimental results reveal that state-of-the-art unlearning algorithms frequently fail to perform effectively under our evaluation framework, particularly when assessed from a feature representation perspective.

2. Related Works

Machine unlearning in image classification. Early research on machine unlearning in neural networks has primarily focused on image classification, leading to the development of various unlearning algorithms with distinct strategies [28]. A widely used approach, Gradient Ascent (GA), maximizes the loss on the forget set to erase its influence, making it one of the most fundamental yet widely adopted techniques in recent studies [6, 13, 15, 31, 37]. Similarly, Fine-tuning achieves unlearning by inducing catastrophic forgetting on forget set, updating the model solely on the retain set [13, 36]. More sophisticated unlearning techniques have been developed: SCRUB [23] employs a knowledge distillation framework to selectively forget knowledge from the forget set while retaining other knowledge. L2UL [6] enhances unlearning by incorporating two regularization terms, mitigating forgetting at both the feature and weight levels when combined with GA. SalUn [12] modifies the most influential parameters through weight saliency, enabling selective unlearning. SCAR [2] leverages metric learning alongside a distillation-based strategy, aligning forget set representations to the nearest incorrect class using the Mahalanobis distance.

Evaluation and analysis of representations. Transfer learning has become a foundational technique in machine

learning, facilitating the adaptation of pre-trained models to diverse downstream tasks [29]. Beyond its practical applications, it is widely used to assess the quality of learned representations. For instance, it has been employed to compare the learned representations of different model architectures [21] and algorithms across various domains, such as self-supervised learning [8, 18] and continual learning [5]. This evaluation is typically performed using metrics such as k -Nearest Neighbors (k -NN) and linear probing, which measure how well the learned representations generalize in various downstream tasks. Centered Kernel Alignment (CKA) [20] has been widely used to compare feature representations across models, providing insights into their structural similarities and differences. Furthermore, t-SNE [33] has been extensively utilized to visualize feature representations, offering an intuitive means to compare and analyze how different models organize learned representations. Our paper makes several contributions that distinguish it from previous machine unlearning studies. First, we highlight the issues with the conventional evaluation methods and setups commonly used in machine unlearning studies, such as logit-based evaluation on small-scale datasets. Second, to address these issues, we propose various forms of representation-based evaluation and introduce a more practical unlearning scenario, namely Top Class-wise Forgetting, supported by a range of experiments. Based on experimental findings, we argue that achieving meaningful progress in unlearning research requires a comprehensive re-evaluation of existing evaluation methods and setups.

3. Analysis Setup and Experimental Results

In this section, we present a comprehensive analysis of machine unlearning methods, focusing on both logit-based and representation-based evaluations in the large-scale setup. We review the classical unlearning evaluation protocols and introduce a new evaluation metric and setup in Sec. 3.1. Then, we introduce the motivation of our approach by highlighting limitations in current evaluation frameworks in Sec. 3.2, introduce our proposed evaluation metric in Sec. 3.3, present experimental findings under large-scale settings from a representation perspective in Sec. 3.4, and show results under top class-wise forgetting scenarios from a transfer learning perspective in Sec. 3.5.

3.1. Analysis Setup

Problem setup and objective of machine unlearning. We define the entire dataset as $\mathcal{D} = \{(x_i, y_i)\}_{i=1}^N$, where x_i represents the input image, y_i denotes its corresponding label, and N is the total number of samples in the dataset. The subset of data targeted for unlearning, referred to as the forget set, is denoted by $\mathcal{D}_f \subset \mathcal{D}$, and consists of samples from specific classes that the model is intended to forget. retain set, denoted by $\mathcal{D}_r = \mathcal{D} \setminus \mathcal{D}_f$, includes all samples

in \mathcal{D} that are not part of the forget set. Additionally, we introduce the test forget set, denoted as $\mathcal{D}_f^{\text{te}}$, which consists of data points from the same classes as \mathcal{D}_f . Similarly, the test retain set, denoted as $\mathcal{D}_r^{\text{te}}$, contains data points from the same classes as \mathcal{D}_r . We assume that an original model θ is trained on the entire dataset \mathcal{D} and is then tasked with unlearning knowledge from \mathcal{D}_f . Note that the goal of machine unlearning is to produce an unlearned model θ_u that retains the knowledge of \mathcal{D}_r while achieving the unlearning of \mathcal{D}_f . Additionally, we consider a retrained model θ_r , which is trained on \mathcal{D}_r from scratch, as an oracle for comparison in the unlearning process.

Logit-based evaluation metrics. As a classical evaluation protocol, unlearning models are evaluated on the following metrics: **Forget Accuracy (FA)**: Measures the accuracy of the unlearned model θ_u on \mathcal{D}_f . **Retain Accuracy (RA)**: Measures the accuracy of the unlearned model θ_u on \mathcal{D}_r . **Test Forget Accuracy (TFA)**: Classification accuracy on the test forget set $\mathcal{D}_f^{\text{te}}$. Similar to FA, this evaluates the model’s ability to forget removed classes beyond the training data. **Test Retain Accuracy (TRA)**: Classification accuracy on the test retain set $\mathcal{D}_r^{\text{te}}$. It indicates how effectively the model’s knowledge generalizes to unseen data of the remaining classes. Following [39], we introduce the **Average GAP of Logit-based Metrics (AGL)**, which quantifies the discrepancy between the given model (*e.g.* the unlearned model θ_u) and the golden standard θ_r . This metric aggregates the logit-based evaluations:

$$\begin{aligned} \text{AGL} = & \left(1 - G(\theta_u, \mathcal{D}_f)\right) \times \left(1 - G(\theta_u, \mathcal{D}_r)\right) \\ & \times \left(1 - G(\theta_u, \mathcal{D}_f^{\text{te}})\right) \times \left(1 - G(\theta_u, \mathcal{D}_r^{\text{te}})\right), \end{aligned} \quad (1)$$

where \mathcal{D}_f , \mathcal{D}_r , $\mathcal{D}_f^{\text{te}}$, and $\mathcal{D}_r^{\text{te}}$ represent the source training datasets and their corresponding test sets, and G computes the classification accuracy differences,

$$G(\theta_u, \mathcal{D}) = |A(\theta_u, \mathcal{D}) - A(\theta_r, \mathcal{D})|,$$

where A represents the classification accuracy on \mathcal{D} .

Representation-based evaluation metrics. To tackle limitations of the logit-based evaluation, we propose using representation-based evaluation. Unlike logit-based evaluation, this approach extracts features from the encoder (*e.g.*, after average pooling in ResNet) and measures the similarity and quality of the representations in unlearned models compared to those in the retrained model. We use the following two metrics for representation-based metrics: First, we use **Centered Kernel Alignment (CKA)** [20] to measure the similarity between the feature representations of θ_u and θ_r , as well as θ_u and θ_o . Second, we measure **k -Nearest Neighbors Accuracy (k -NN)** [9] to assess the representational quality of θ_u . We employ a k -NN classifier, which takes features of the test data from a model and performs

classification based on the neighborhood features. Additionally, we also employ t-SNE [33] to visualize feature distributions. More details on these methods are provided in Fig. A. 2 in the Appendix.

Model and datasets. To ensure a more accurate and meaningful evaluation of unlearning algorithms considering real-world scenarios, we employed the ResNet-50 [17] model pre-trained on the ImageNet-1k [10] as the basic setting.

Unlearning baselines. We evaluate several representative machine unlearning algorithms in classification, which can be categorized into two groups: 1) Unlearning without \mathcal{D}_r , including Gradient Ascent (GA)[32], Random Labeling (RL)[14], Pseudo Labeling (PL)[7], and SalUn[12]; and 2) unlearning with \mathcal{D}_r , including DUCK [11], Contrastive Unlearning (CU) [38], SCRUB [23], and SCAR [2]. Note that SalUn and SCAR are known as current state-of-the-art methods in each category. A more detailed explanation of each baseline can be found in Sec. A in the Appendix.

Unlearning scenarios. In our experiments and analysis, we consider two unlearning scenarios. The first is Random- N Class-wise Forgetting, where we randomly select N classes to remove. This scenario is a standard approach to evaluate unlearning algorithms. To provide a more comprehensive assessment, we also introduce a second scenario, Top- N Class-wise Forgetting, in which we specifically target classes that exhibit semantic similarity to the downstream task classes. The selection of N classes is based on their relevance to the downstream task.

3.2. Motivation: Why Do We Need Representation-Based Metrics?

Current machine unlearning algorithms predominantly rely on logit-based evaluation metrics to assess their effectiveness. These algorithms aim to achieve classification accuracy similar to models trained only on retain set (θ_r), and based on these metrics, they are considered to have successfully accomplished unlearning. However, this evaluation raises a critical research question: Do existing unlearning evaluations adequately reflect successful unlearning from a representation perspective?

To explore this question, we investigate whether unlearned models (θ_u) exhibit feature representations that are more similar to those of the retrained model (θ_r) while remaining significantly different from the original model (θ_o). To do this, we randomly select 100 forget classes from the 1,000 classes in ImageNet-1k and perform unlearning using baseline algorithms.

t-SNE visualization. We first conducted an analysis on several unlearning baselines using t-SNE in Fig. 3, which provides a visualization of feature embeddings in a lower-dimensional space. While several unlearning algorithms (GA, RL, SalUn) achieve superior performance on logit-based evaluation metrics in small-scale settings, Fig. 3 re-

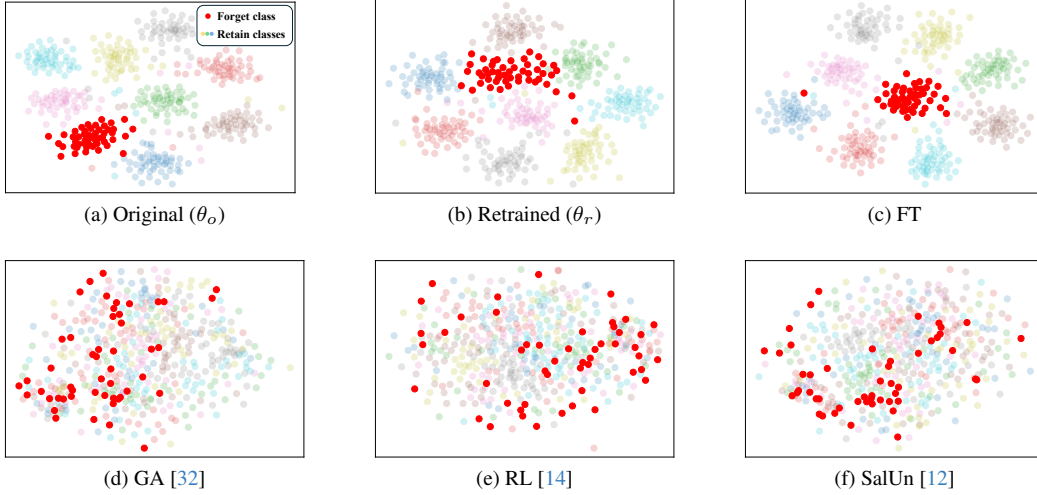


Figure 3. We visualize the feature representations from the original (θ_o), retrained (θ_r), and unlearned models (θ_u) on a subset of ImageNet-1k using ResNet-50. Unlike the retrained model (θ_r), which serves as the gold standard, the forget classes (highlighted in red) in the existing unlearning baselines (e.g., (d), (e), and (f)) are dispersed throughout the entire class distribution. This dispersion indicates that these unlearning approaches fail to effectively isolate the forget classes.

veals several important findings. First, (a) Original (θ_o), (b) Retrain (θ_r), and (c) Fine-Tuning (FT) models exhibit feature representations where each class forms distinct clusters. We expect that an effective unlearning algorithm should ideally produce feature representations similar to those of (b) (θ_r). However, Figures (d)-(f) reveal that these approaches induce substantial collapse in feature representations, which deviate considerably from those of θ_r , exposing a critical inconsistency. For t-SNE visualization results of other algorithms, see Fig. A in the Appendix.

CKA analysis. In Fig. 4, we compare the Centered Kernel Alignment (CKA) similarity values between the unlearned (θ_u) and retrained (θ_r) models (on the y-axis) against those between the unlearned and original (θ_o) models (on the x-axis), using ImageNet-1k. Note that CKA quantifies the representational similarity between different models, providing a measure of how similarly two models “see” or interpret the given data. Intuitively, if two models are aligned in their feature representations, they can be considered to share a similar perspective on the data. In the context of successful unlearning, we expect the CKA similarity between the unlearned and retrained models to be higher than that between the unlearned and original models. However, our findings reveal a critical issue: all unlearning baselines show a higher similarity to the original model’s representations than to the retrained model’s representations. In fact, certain baselines, such as GA, SalUn, and RL, exhibit very low similarity to both the original and retrained models.

Why does the unlearned model maintain high similarity to the original model? Several unlearning baselines show high logit-based metric scores (i.e., minimal deviation from the retrained model) in this experimental setup, while still maintaining a strong resemblance to the original

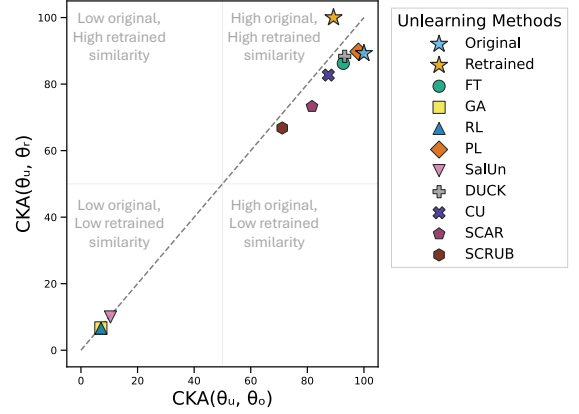


Figure 4. CKA similarity analysis of various unlearning algorithms. The x-axis shows the similarity to the original model, and the y-axis represents the similarity to the retrained model. In an ideal scenario, algorithms should be positioned near the top-left corner, indicating high similarity to the retrained model and relatively low similarity to the original model. However, most algorithms exhibit a high similarity to the original model and limited alignment with the retrained model, suggesting that the transformation of representations during unlearning is suboptimal.

model’s representations. We hypothesize that this occurs because unlearning algorithms tend to focus on modifying the final layer to optimize logit-based metrics, while leaving earlier representational layers largely unchanged. In Fig. 5, we compare the CKA similarities between unlearned models, where either all layers are tuned (θ_u) or only the final layer is tuned (θ_u^{last}), alongside the gap in logit-based AGL (Eq. 1) scores (y-axis). Ideally, the CKA similarity should be low (low x-values), which would correspond to a higher gap in AGL scores (high y-values). However, θ_u shows high similarity to θ_u^{last} while presenting a relatively small gap in

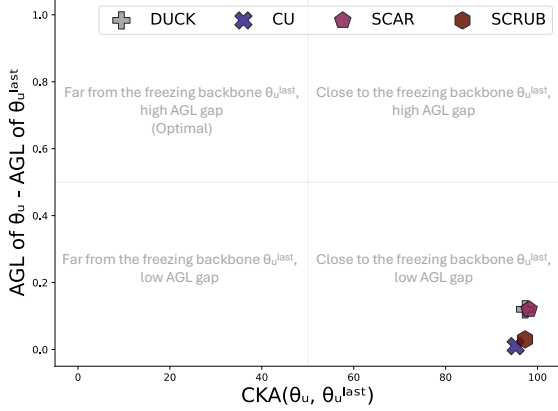


Figure 5. The X-axis depicts the feature similarity between unlearned models with tuning all layers layer (θ_u) versus only the final layer (θ_u^{last}). Y-axis represents the gap in AGL scores between θ_u and θ_u^{last} . The results indicate that θ_u modifies only the last layer while maintaining a similar representation space.

AGL, demonstrating a crucial limitation in the current evaluation approach.

In summary, the results from both t-SNE and CKA analyses highlight a key limitation in relying solely on logit-based metrics for unlearning evaluation. While some algorithms show high logit-based performance, their feature representations remain too similar to the original model, indicating insufficient unlearning. This underscores the need for representation-based metrics, which can more effectively capture the changes in feature representations and provide a more accurate measure of unlearning effectiveness, especially in large-scale, real-world applications.

3.3. The Proposed Unified Evaluation Framework

To establish a rigorous and comprehensive evaluation of unlearning algorithms, we propose a unified framework that integrates both logit-based and representation-based metrics. This framework enables a more holistic assessment of unlearning performance by capturing both **Feature Similarity** and **Feature Transferability**—two fundamental aspects of an unlearned model’s behavior. First, **Feature Similarity** quantifies the alignment of feature representations between on the same dataset. To measure this, we employ Centered Kernel Alignment (CKA), which provides a robust similarity measure between the learned representations of both models. Second, Feature Transferability evaluates how well the unlearned model’s learned representations generalize to downstream tasks. We assess this by applying a k -Nearest Neighbors (k -NN) classifier to the encoder’s output features and assess performance on several downstream datasets. This allows us to measure how well features generalize beyond the original training distribution.

Unified metric. To establish a comprehensive evaluation of unlearning algorithms, we propose a unified measure that

integrates both logit-based and representation-based evaluations. For representation-based evaluation, we use diverse downstream datasets, \mathcal{D}_{down} , which differ from the original training distribution (*e.g.*, ImageNet-1k). Inspired by transfer learning evaluation protocols [29], this approach enables us to assess both the quality and generalizability of learned representations. Specifically, we evaluate models on three downstream datasets: Office-Home [34], CUB [35], and DomainNet-126 [30]. Further details on these datasets can be found in Sec A.3 in the Appendix.

To formally quantify representation changes, we define two key metrics: First, G_{kNN} measures the difference in classification accuracy (A^k) of a k -NN classifier between θ_u and θ_r using a downstream dataset:

$$G_{kNN}(\theta_u, \mathcal{D}_{down}) = |A^k(\theta_u, \mathcal{D}_{down}) - A^k(\theta_r, \mathcal{D}_{down})|.$$

This metric evaluates the transfer learning ability of the given model’s encoder compared to that of the retrained model. In addition, we quantify the representational similarity between the given and retrained models for the given downstream dataset, by using CKA_{AGR} :

$$CKA_{AGR}(\theta_u, \mathcal{D}_{down}),$$

which measures the representational similarity between the given and retrained models over the downstream dataset.

Using these metrics, we define the Average GAP of Representation-based metrics (AGR) as:

$$AGR = \left(1 - G_{kNN}(\theta_u, \mathcal{D}_{down})\right) \times CKA_{AGR}(\theta_u, \mathcal{D}_{down}).$$

This formulation balances the impact of both feature divergence and transferability degradation, providing a more nuanced measure of unlearning effectiveness in a representation perspective.

Finally, we introduce a unified evaluation measure, $H-LR$, which harmonizes both logit-based (AGL) and representation-based (AGR) metrics into a single, unified evaluation measure:

$$H-LR = \frac{2}{\frac{1}{AGL} + \frac{1}{AGR}}.$$

This harmonic mean formulation ensures that both classification performance and representational divergence are jointly considered, making $H-LR$ a robust and comprehensive metric for evaluating unlearning algorithms.

3.4. Re-evaluation of Unlearning Baselines under Large-Scale Unlearning Scenarios

In this section, we present experimental results for random class-wise unlearning in large-scale settings, evaluating both logit-based and representation-based performance.

Small-scale vs. large-scale unlearning. Several unlearning algorithms have demonstrated strong performance in

Table 1. The comparison of unlearning performance across different θ_u on ImageNet-1K under random 100 class-wise forgetting. The blue numbers represent the gap from θ_r , demonstrating the efficacy of different unlearning strategies.

Method	ImageNet-1K					AGL \uparrow	Office-Home	CUB	DomainNet-126	Office-Home	CUB	DomainNet-126	CKA(θ_u, θ_r) >		
	FA	RA	TFA	TRA	Avg. Gap		k -NN						AGR \uparrow	H-LR \uparrow	CKA(θ_u, θ_r)
Original	79.2 (79.2)	80.1 (4.1)	76.1 (76.1)	76.5 (0.9)	40.1	-	80.3 (3.0)	43.4 (6.5)	84.0 (2.0)	89.8 (10.2)	82.1 (17.9)	81.8 (18.2)	-	-	\times
Retrained	0.0 (0.0)	76.0 (0.0)	0.0 (0.0)	75.6 (0.0)	0.0	1.00	77.3 (0.0)	36.9 (0.0)	82.0 (0.0)	100.0 (0.0)	100.0 (0.0)	100.0 (0.0)	1.00	1.00	\checkmark
FT	9.9 (9.9)	79.5 (3.5)	10.5 (10.5)	76.0 (0.4)	6.1	0.78	78.4 (1.1)	39.0 (2.1)	81.6 (0.4)	87.6 (12.4)	79.0 (21.0)	79.9 (20.1)	0.81	0.79	\times
GA	1.5 (1.5)	11.4 (64.6)	1.5 (1.5)	11.3 (64.3)	33.0	0.12	29.7 (47.6)	10.4 (26.5)	42.2 (39.8)	8.3 (91.7)	9.8 (90.2)	10.2 (89.8)	0.06	0.08	\times
RL	6.3 (6.3)	14.3 (62.7)	5.5 (5.5)	13.0 (62.6)	34.3	0.12	44.0 (33.3)	8.0 (28.9)	35.2 (46.8)	6.3 (93.7)	5.8 (94.2)	4.7 (95.3)	0.04	0.06	\times
PL	1.0 (1.0)	79.5 (3.5)	1.0 (1.0)	76.9 (0.9)	1.6	0.94	80.3 (3.0)	43.3 (6.4)	84.0 (2.0)	91.6 (8.4)	84.7 (15.3)	84.5 (15.5)	0.84	0.89	\times
SalUn	10.4 (10.4)	19.7 (56.3)	9.3 (9.3)	19.1 (56.5)	32.8	0.15	38.5 (38.8)	8.0 (28.9)	42.5 (39.5)	9.7 (90.3)	8.0 (92.0)	8.5 (91.5)	0.06	0.09	\times
DUCK	0.9 (0.9)	74.6 (1.4)	0.9 (0.9)	74.5 (1.1)	1.1	0.96	79.8 (2.5)	39.0 (2.1)	82.5 (0.7)	90.7 (9.3)	83.2 (16.8)	84.9 (15.1)	0.85	0.90	\times
CU	2.1 (2.1)	73.9 (2.1)	2.2 (2.2)	73.3 (2.3)	2.2	0.92	75.8 (1.5)	33.9 (3.0)	80.1 (1.9)	85.6 (14.4)	75.9 (24.1)	76.1 (23.9)	0.78	0.84	\times
SCAR	4.2 (4.2)	80.5 (4.5)	3.9 (3.9)	77.4 (1.8)	3.6	0.87	78.0 (0.7)	42.8 (5.9)	83.1 (1.1)	74.2 (25.8)	65.4 (34.6)	58.8 (41.2)	0.64	0.74	\times
SCRUB	1.1 (1.1)	67.3 (8.7)	1.1 (1.1)	65.7 (9.9)	5.2	0.80	74.7 (2.6)	42.2 (5.3)	80.9 (1.1)	68.9 (51.1)	63.8 (36.2)	52.8 (47.2)	0.60	0.69	\times

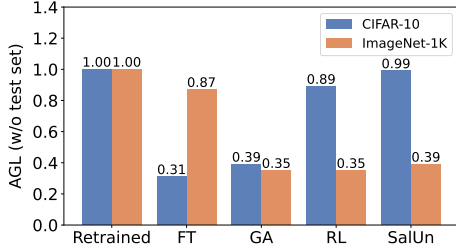


Figure 6. AGL results for unlearning experiments on pretrained ResNet-50 models using CIFAR-10 and ImageNet-1k. We conduct unlearning on a pretrained model for one randomly selected class from CIFAR-10 and 100 randomly selected classes from ImageNet-1k. Notably, following the evaluation protocol of SalUn, we exclude test set accuracy when calculating AGL.

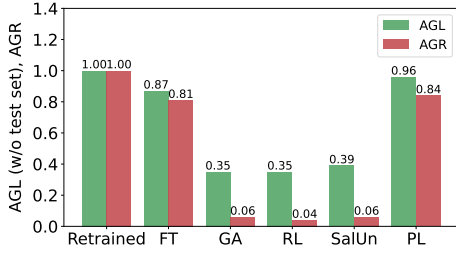


Figure 7. AGL and AGR results for unlearning experiments on pretrained ResNet-50 models using ImageNet-1k. We conduct unlearning on a pretrained model for 100 randomly selected classes from ImageNet-1k and report the corresponding AGL and AGR values. Notably, following the evaluation protocol of SalUn, we exclude test set accuracy when computing AGL.

small-scale settings, as evaluated by logit-based metrics. As shown in Fig. 6, both RL and SalUn achieve superior AGL on CIFAR-10. However, the figure also clearly highlights a significant performance degradation in ImageNet-1k, underscoring the challenges associated with scaling unlearning algorithms to larger datasets.

Fig. 7 further presents both AGL and AGR scores in large-scale unlearning experiments. AGL scores, measured using ImageNet-1k, are accompanied by averaged AGR scores, which are calculated using multiple downstream datasets, $\mathcal{D}_{\text{down}}$. This figure emphasizes the limitations of both existing unlearning algorithms and the evaluation

methods currently in use. First, three algorithms—GA, RL, and SalUn—demonstrate a significant drop in performance in the large-scale unlearning scenario. Second, all baseline algorithms consistently exhibit low AGR compared to AGL, indicating their failure to effectively unlearn from a representational perspective.

Experimental results in large-scale unlearning. Table 1 presents the experimental results for all baselines and evaluation methods in large-scale unlearning scenarios. Through logit-based evaluation and AGL scores, we observe that PL (which does not use D_r) achieves performance comparable to, or even surpassing, state-of-the-art algorithms that do utilize D_r (i.e., DUCK, CU, SCAR, and SCRUB). This result marks a notable departure from the trends observed in small-scale unlearning experiments [2, 11, 23, 26]. In representation-based evaluation (measured by AGR), PL consistently outperforms other algorithms, achieving superior H-LR among the baselines. These results challenge prior expectations, showing that many state-of-the-art algorithms, such as SalUn, SCAR, and SCRUB, degrade in large-scale unlearning scenarios, performing worse from both logit and representation perspectives.

3.5. Experiments on Top Class-wise Forgetting

Why top class-wise forgetting is necessary? In the random-class forgetting scenario, the CKA similarity between the retrained and original models reaches a high value of 88%, as shown in Fig. 4. We hypothesize that this high similarity arises from the presence of multiple alternative classes within ImageNet, which may preserve similar representational knowledge. Consequently, this results in a significant overlap between both the models, presenting challenges in verifying the effectiveness of unlearning.

To address this, we propose a novel top class-wise forgetting approach, where forgotten classes are selected based on semantic similarity criteria. This ensures that no alternative classes with similar representations remain in the retained data, leading to a substantial difference between θ_r and θ_o . As shown in Fig. B in the Appendix, this approach minimizes CKA similarity, thereby facilitating a more reliable and straightforward evaluation of unlearning.

In selecting semantically similar classes, we leverage

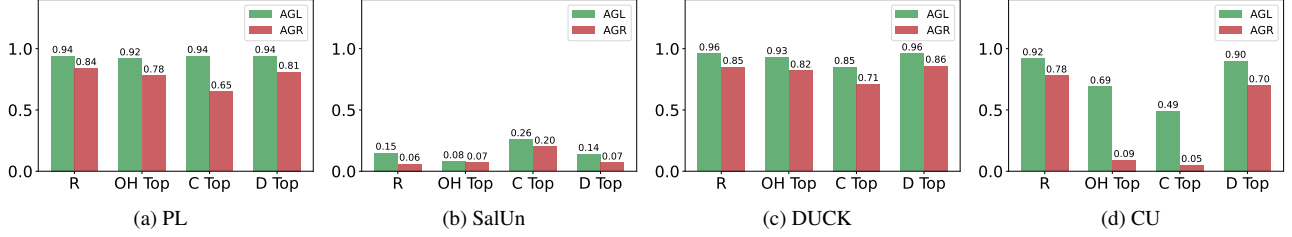


Figure 8. Comparison of AGL and AGR across different unlearning baselines, using Random (R), Office-Home (OH), CUB (C), and DomainNet-126 (D) to select semantically similar 100 classes for top-class wise unlearning.

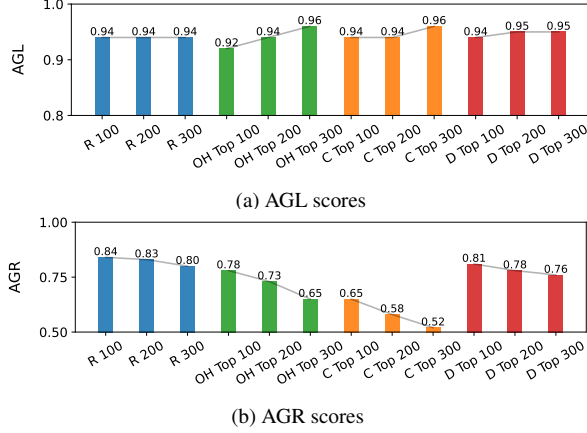


Figure 9. AGL and AGR scores in Random and Top class-wise forgetting scenarios on PL. (a) AGL score archives consistently high in all settings. (b) AGR scores decrease, as the number of forgetting classes increases. This is more evident in top class-wise forgetting, where θ_r has a low similarity to θ_o .

transfer learning techniques. Specifically, our top class-wise forgetting approach defines the forget set as the classes most similar to those in downstream datasets. We rank the classes and select the top 100 most similar ones for the forget set. For example, in the case of Office-Home, which consists of 65 classes, we identify the most similar classes to this dataset as the forget set. To complete the unlearning scenario, we extend the next 35 most similar classes, creating a 100-class forget set. If unlearning is successful, we expect to observe corresponding changes in performance on related classes in downstream tasks.

Random vs. Top class-wise forgetting. We conduct extensive experiments comparing random and top class-wise unlearning across several datasets. The results are presented in Fig. 8. An ideal unlearning should show minimal gaps in both AGL and AGR, regardless of unlearning scenarios. As shown in Fig. 8a, PL consistently achieves high and comparable AGL scores across all settings. However, its AGR scores exhibit significant variation depending on the unlearning scenario, highlighting its weakness in top class-wise unlearning. Furthermore, both SalUn (Fig. 8b) and CU (Fig. 8d) show considerably degraded performance in terms of both AGL and AGR in most top class-wise unlearning cases. Additionally, even though DUCK (Fig. 8c) achieves

relatively stable performance compared to other baselines, we observe that most unlearning methods exhibit significantly lower AGR scores compared to the corresponding AGL scores, especially in the CUB Top case.

Need for considering both AGL and AGR, respectively. Fig. 9a reveals that unlearning algorithms exhibit unexpected behaviors, which become evident when considering both AGR and AGL scores. Despite PL and DUCK often showing little disparity between these scores, there is an inherent need to assess these measures independently to fully understand the performance of the algorithms. To demonstrate this, we extended the evaluation of PL by performing experiments with 100 to 300 top class-wise unlearning classes. As the number of classes to forget increases, particularly in top class-wise forgetting, the nearest classes diverge significantly from the original ones. Fig. 9 illustrates that AGL scores remain largely unaffected by the number of forgetting classes. However, AGR scores notably decrease as the number of forgotten classes rises, indicating that PL retains substantial similarity to θ_o 's representation while diverging from the retrained model. These findings not only highlight the discrepancy between the unlearning performed by these algorithms and the expected results but also emphasize the need for our proposed multi-faceted evaluation approach to better capture the effect of unlearning. Fig. C in the appendix shows the similar results on DUCK.

Note that we report detailed experimental and additional experimental results in Tables B-F in the Appendix.

4. Conclusion

This work introduces a new representation-based evaluation framework for large-scale unlearning, addressing the limitations of traditional logit-based metrics used in small-scale settings. Our experiments reveal that current unlearning algorithms struggle to scale in real-world scenarios, and logit-based metrics fail to capture the full impact of unlearning on model representations. Additionally, we show that random-class forgetting may not be enough to evaluate unlearning algorithms, while our top class-wise forgetting provides a more reliable and interpretable evaluation. These findings highlight the need for more robust and scalable unlearning methods, evaluated through our proposed framework.

References

- [1] Yoshua Bengio, Yann Lecun, and Geoffrey Hinton. Deep learning for ai. *Communications of the ACM*, 64(7):58–65, 2021. 1
- [2] Jacopo Bonato, Marco Cotogni, and Luigi Sabetta. Is retain set all you need in machine unlearning? restoring performance of unlearned models with out-of-distribution images. In *European Conference on Computer Vision (ECCV)*, 2024. 1, 2, 3, 4, 7, 11, 16
- [3] Yinzhi Cao and Junfeng Yang. Towards making systems forget with machine unlearning. In *2015 IEEE Symposium on Security and Privacy*, pages 463–480, 2015. 1
- [4] Nicholas Carlini, Florian Tramer, Eric Wallace, Matthew Jagielski, Ariel Herbert-Voss, Katherine Lee, Adam Roberts, Tom Brown, Dawn Song, Ulfar Erlingsson, et al. Extracting training data from large language models. In *30th USENIX Security Symposium (USENIX Security 21)*, pages 2633–2650, 2021. 1
- [5] Sungmin Cha, Jihwan Kwak, Dongsub Shim, Hyunwoo Kim, Moontae Lee, Honglak Lee, and Taesup Moon. Towards more objective evaluation of class incremental learning: Representation learning perspective. *arXiv preprint arXiv:2206.08101*, 2022. 3
- [6] Sungmin Cha, Sungjun Cho, Dasol Hwang, Honglak Lee, Taesup Moon, and Moontae Lee. Learning to unlearn: Instance-wise unlearning for pre-trained classifiers. *arXiv preprint arXiv:2301.11578*, 2024. AAAI 2024 camera ready version, Available at <https://doi.org/10.48550/arXiv.2301.11578>. 1, 2, 3
- [7] Huiqiang Chen, Tianqing Zhu, Xin Yu, and Wanlei Zhou. Machine unlearning via null space calibration. In *Proceedings of the 33rd International Joint Conference on Artificial Intelligence (IJCAI)*, 2024. 4, 11, 16
- [8] Ting Chen, Simon Kornblith, Mohammad Norouzi, and Geoffrey Hinton. A simple framework for contrastive learning of visual representations. In *International conference on machine learning*, pages 1597–1607. PMLR, 2020. 3
- [9] Thomas Cover and Peter Hart. Nearest neighbor pattern classification. *IEEE transactions on information theory*, 13(1): 21–27, 1967. 4
- [10] Jia Deng, Wei Dong, Richard Socher, Li-Jia Li, Kai Li, and Li Fei-Fei. Imagenet: A large-scale hierarchical image database. *2009 IEEE conference on computer vision and pattern recognition*, pages 248–255, 2009. 1, 4
- [11] Yujie Du, Kai Zhang, and Lin Wang. Distance-based unlearning through centroid kinematics (duck). *arXiv preprint arXiv:2312.02052*, 2023. 4, 7, 11, 16
- [12] Chongyu Fan, Jiancheng Liu, Yihua Zhang, Eric Wong, Dennis Wei, and Sijia Liu. Salun: Empowering machine unlearning via gradient-based weight saliency in both image classification and generation. *arXiv preprint arXiv:2310.12508*, 2024. 1, 2, 3, 4, 5, 11, 16
- [13] Aditya Golatkar, Alessandro Achille, and Stefano Soatto. Eternal sunshine of the spotless net: Selective forgetting in deep networks. In *Proceedings of the IEEE/CVF Conference on Computer Vision and Pattern Recognition*, pages 9304–9312, 2020. 3
- [14] Aditya Golatkar, Alessandro Achille, and Stefano Soatto. Eternal sunshine of the spotless net: Selective forgetting in deep networks. *arXiv preprint arXiv:1911.04933*, 2020. Accepted at CVPR 2020, Available at <https://doi.org/10.48550/arXiv.1911.04933>. 1, 4, 5, 11, 16
- [15] Laura Graves, Vineel Nagisetty, and Vijay Ganesh. Amnesiac machine learning. In *Proceedings of the AAAI Conference on Artificial Intelligence*, pages 11516–11524, 2021. 3
- [16] Chuan Guo, Tom Goldstein, Awni Hannun, and Laurens Van Der Maaten. Certified data removal from machine learning models. In *Proceedings of the 37th International Conference on Machine Learning*, pages 3832–3842, 2020. 1
- [17] Kaiming He, Xiangyu Zhang, Shaoqing Ren, and Jian Sun. Deep residual learning for image recognition. *Proceedings of the IEEE conference on computer vision and pattern recognition*, pages 770–778, 2016. 1, 4
- [18] Kaiming He, Haoqi Fan, Yuxin Wu, Saining Xie, and Ross Girshick. Momentum contrast for unsupervised visual representation learning. In *Proceedings of the IEEE/CVF conference on computer vision and pattern recognition*, pages 9729–9738, 2020. 3
- [19] Dongjae Jeon, Wonje Jeung, Taeheon Kim, Albert No, and Jonghyun Choi. An information theoretic evaluation metric for strong unlearning. *arXiv preprint arXiv:2405.17878*, 2024. 12
- [20] Simon Kornblith, Mohammad Norouzi, Honglak Lee, and Geoffrey Hinton. Similarity of neural network representations revisited. In *Proceedings of the 36th International Conference on Machine Learning (ICML)*, pages 3519–3529. PMLR, 2019. 2, 3, 4, 12
- [21] Simon Kornblith, Jonathon Shlens, and Quoc V Le. Do better imagenet models transfer better? In *Proceedings of the IEEE/CVF conference on computer vision and pattern recognition*, pages 2661–2671, 2019. 3
- [22] Alex Krizhevsky and Geoffrey Hinton. Learning multiple layers of features from tiny images. Technical Report 0, University of Toronto, Toronto, Ontario, 2009. 1
- [23] Meghdad Kurmanji, Peter Triantafillou, Jamie Hayes, and Eleni Triantafillou. Towards unbounded machine unlearning. In *37th Conference on Neural Information Processing Systems (NeurIPS)*, 2023. 1, 2, 3, 4, 7, 11, 16
- [24] Ze Liu, Yutong Lin, Yue Cao, Han Hu, Yixuan Wei, Zheng Zhang, Stephen Lin, and Baining Guo. Swin transformer: Hierarchical vision transformer using shifted windows. *Proceedings of the IEEE/CVF International Conference on Computer Vision (ICCV)*, pages 10012–10022, 2021. 13
- [25] Zhuang Liu, Hanzi Mao, Chao-Yuan Wu, Christoph Feichtenhofer, Trevor Darrell, and Saining Xie. A convnet for the 2020s. *Proceedings of the IEEE/CVF Conference on Computer Vision and Pattern Recognition (CVPR)*, pages 11976–11986, 2022. 1, 13
- [26] Ananth Mahadevan and Michael Mathioudakis. Certifiable machine unlearning for linear models. *ArXiv*, abs/2106.15093, 2021. 1, 7

- [27] Alessandro Mantelero. The eu proposal for a general data protection regulation and the roots of the ‘right to be forgotten’. *Computer Law & Security Review*, 29(3):229–235, 2013. [1](#)
- [28] Thanh Tam Nguyen, Thanh Trung Huynh, Zhao Ren, Phi Le Nguyen, Alan Wee-Chung Liew, Hongzhi Yin, and Quoc Viet Hung Nguyen. A survey of machine unlearning. *arXiv preprint arXiv:2209.02299*, 2022. [1](#), [3](#)
- [29] Sinno Jialin Pan and Qiang Yang. A survey on transfer learning. *IEEE Transactions on knowledge and data engineering*, 22(10):1345–1359, 2010. [3](#), [6](#)
- [30] Xingchao Peng, Ziwei Bai, Xiang Xia, Zhangying Huang, Kate Saenko, Bo Wang, and Ranran Yu. Moment matching for multi-source domain adaptation. In *Proceedings of the IEEE/CVF International Conference on Computer Vision*, pages 1406–1415, 2019. [6](#), [12](#)
- [31] Ayush K Tarun, Vikram S Chundawat, Murari Mandal, and Mohan Kankanhalli. Fast yet effective machine unlearning. *arXiv preprint arXiv:2111.08947*, 2021. [3](#)
- [32] Anvith Thudi, Gabriel Deza, Varun Chandrasekaran, and Nicolas Papernot. Unrolling sgd: Understanding factors influencing machine unlearning. In *2022 IEEE 7th European Symposium on Security and Privacy (EuroS&P)*, pages 303–319. IEEE, 2022. [1](#), [4](#), [5](#), [11](#), [16](#)
- [33] Laurens Van der Maaten and Geoffrey Hinton. Visualizing data using t-sne. *Journal of machine learning research*, 9(11), 2008. [3](#), [4](#)
- [34] Hemanth Venkateswara, Joseph Eusebio, Shayok Chakraborty, and Sethuraman Panchanathan. Deep hashing network for unsupervised domain adaptation. In *Proceedings of the IEEE conference on computer vision and pattern recognition*, pages 5018–5027, 2017. [6](#), [12](#)
- [35] Catherine Wah, Steve Branson, Peter Welinder, Pietro Perona, and Serge Belongie. The caltech-ucsd birds-200-2011 dataset. Technical report, California Institute of Technology, 2011. [6](#), [12](#)
- [36] Alexander Warnecke, Lukas Pirch, Christian Wressnegger, and Konrad Rieck. Machine unlearning of features and labels. *arXiv preprint arXiv:2108.11577*, 2021. [3](#)
- [37] Jingwen Ye, Yifang Fu, Jie Song, Xingyi Yang, Songhua Liu, Xin Jin, Mingli Song, and Xinchao Wang. Learning with recoverable forgetting. *arXiv preprint arXiv:2207.08224*, 2022. [3](#)
- [38] Qiuchen Zhang, Carl Yang, Jian Lou, Li Xiong, et al. Contrastive unlearning: A contrastive approach to machine unlearning. *arXiv preprint arXiv:2401.10458*, 2024. [4](#), [11](#), [16](#)
- [39] Kairan Zhao, Meghdad Kurmanji, George-Octavian Bărbulescu, Eleni Triantafillou, and Peter Triantafillou. What makes unlearning hard and what to do about it. *Advances in Neural Information Processing Systems*, 37: 12293–12333, 2024. [4](#)

A. Detail Descriptions

A.1. Unlearning Baselines

We divide unlearning baselines into two categories based on whether they use the retain set (\mathcal{D}_r): (i) baselines without \mathcal{D}_r , and (ii) baselines with \mathcal{D}_r . The details of these algorithms are as follows.

Unlearning w/o \mathcal{D}_r . In this section, baselines aim to remove information using only \mathcal{D}_f without referencing the retain set. While this reduces time complexity and privacy risk, it often sacrifices some accuracy on retain set.

Gradient Ascent (GA) [32]. GA forces the model to misclassify \mathcal{D}_f by maximizing the loss on forget samples. For a set of forget tuples $\{(x_i, y_i)\} \subset \mathcal{D}_f$, GA updates model parameters θ_o with the cross-entropy loss ℓ :

$$\theta \leftarrow \theta + \eta \nabla_{\theta} \left[\sum_{(x_i, y_i) \in \mathcal{D}_f} \ell(f_{\theta}(x_i), y_i) \right]. \quad (2)$$

Random Labeling (RL) [14]. RL discards ground-truth labels for forget set and replaces each y_i with a label y_i^{rand} sampled from other classes:

$$\min_{\theta} \sum_{(x_i, y_i^{\text{rand}}) \in \mathcal{D}_f} \ell(f_{\theta}(x_i), y_i^{\text{rand}}). \quad (3)$$

By training on random labels for \mathcal{D}_f , the network forgets the original associations.

Pseudo Labeling (PL [7]). PL ensures that \mathcal{D}_f is unlearned in a manner that minimizes noise. For each sample $x_i \in \mathcal{D}_f$, the original model θ_o assigns a pseudo-label y'_i , representing the class with the highest predicted probability after excluding forget set. The unlearning objective is defined as:

$$\min_{\theta} \sum_{(x_i, y'_i) \in \mathcal{D}_f} \ell(f_{\theta}(x_i), y'_i). \quad (4)$$

where y'_i is the pseudo-label and ℓ denotes the cross-entropy loss. Unlike random or heuristic labeling methods, Pseudo-Labeling ensures that \mathcal{D}_f is mapped to semantically similar classes, preserving the decision boundary of the model.

SalUn [12]. SalUn restricts unlearning updates to only those parameters deemed salient for classifying \mathcal{D}_f . Let $\theta_s \subseteq \theta$ be the parameter subset. Then the update is

$$\theta_s \leftarrow \theta_s - \eta \nabla_{\theta_s} \sum_{(x_i, y_i) \in \mathcal{D}_f} \ell(f_{\theta}(x_i), y_i). \quad (5)$$

This targets \mathcal{D}_f knowledge at the parameter level while minimally disturbing the rest of the network.

Unlearning w/ \mathcal{D}_r . Several baselines utilize \mathcal{D}_r as using only \mathcal{D}_f often fails to preserve the knowledge of \mathcal{D}_r . Baselines in this category incorporate training or distillation on the retain set, thereby improving utility for the retain set.

DUCK [11]. DUCK employs a distance-based metric learning objective to destroy class cues for \mathcal{D}_f . Suppose each valid class $c \neq y_i$ has a centroid \mathbf{m}_c . For each forget set (x_i, y_i) , DUCK shifts $f_{\theta}(x_i)$ (the feature embedding) to the nearest incorrect centroid:

$$\min_{\theta} \sum_{(x_i, y_i) \in \mathcal{D}_f} \text{dist}(f_{\theta}(x_i), \mathbf{m}_{c^*}), \quad (6)$$

$$c^* = \arg \min_{c \neq y_i} \text{dist}(f_{\theta}(x_i), \mathbf{m}_c).$$

In doing so, the feature space for forget classes is pushed into the incorrect boundary.

Contrastive Unlearning (CU) [38]. CU uses a contrastive objective to decouple the forget set from the retain set in embedding space. Though one can implement CU without \mathcal{D}_r explicitly in every step (e.g., by approximating distances), it is often more effective when \mathcal{D}_r is used to preserve the retain set.

SCRUB [23]. SCRUB uses a teacher–student paradigm. The original model (teacher) provides knowledge about \mathcal{D}_r , but its information on \mathcal{D}_f is filtered. If $f_{\theta}(x)$ is the teacher’s feature, and $f_{\theta_u}(x)$ is the student’s, SCRUB trains θ_u to match the teacher’s logits on \mathcal{D}_r , while removing any relevant signals from \mathcal{D}_f . One can write a selective distillation objective:

$$\max_{\theta_u} \sum_{(x_j, y_j) \in \mathcal{D}_f} d(f_{\theta_u}(x_j), f_{\theta}(x_j)) + \min_{\theta_u} \sum_{(x_j, y_j) \in \mathcal{D}_r} d(f_{\theta_u}(x_j), f_{\theta}(x_j)). \quad (7)$$

with an additional mechanism that blocks or penalizes the student’s copying of the teacher’s information for classes in \mathcal{D}_f .

SCAR [2]. SCAR exploits a distance-based realignment for \mathcal{D}_f , pushing their features toward incorrect classes to erase the original boundary, which preserves the representation for \mathcal{D}_r via distillation or cross-entropy minimizing these terms:

$$\sum_{(x_i, y_i) \in \mathcal{D}_f} \text{dist}(f_{\theta}(x_i), \mathbf{m}_{c^*}) + \sum_{(x_j, y_j) \in \mathcal{D}_r} \ell(f_{\theta}(x_j), y_j). \quad (8)$$

where \mathbf{m}_{c^*} is again an incorrect-class centroid. We use retained classes for \mathcal{D}_r in this paper.

A.2. Representation-Based Metrics

Centered Kernel Alignment (CKA). A successful unlearning algorithm can be identified if the feature representations of the unlearned model align closely with those of

the retrained model, which serves as the oracle. To quantitatively evaluate this alignment, we employ Centered Kernel Alignment (CKA) [20], a robust metric for assessing the similarity between feature representations. CKA operates by comparing the normalized Gram matrices of two sets of feature embeddings. Specifically, the CKA between two Gram matrices K and L is defined as:

$$\text{CKA}(K, L) = \frac{\|\text{HSIC}(K, L)\|_F^2}{\|\text{HSIC}(K, K)\|_F^2 \cdot \|\text{HSIC}(L, L)\|_F^2}, \quad (9)$$

where K and L represent the Gram matrices of the two feature representations, and HSIC denotes the Hilbert-Schmidt independence criterion. By applying CKA, we measure the similarity between the feature representations of θ_u (the unlearned model) and θ_o (the original model), θ_r (the retrained model) across various downstream datasets. Note that higher CKA values indicate a greater degree of alignment, suggesting that the unlearned model retains the desired feature representations after unlearning.

k -Nearest Neighbors (k -NN). To evaluate the transferability of the unlearned model, we leverage k -NN. Feature embeddings are extracted from the unlearned model, θ_u , by feeding it the downstream data. These embeddings are then split, with 80% used to train a k -NN classifier and the remaining 20% used for testing. For each test sample, the classifier assigns a label based on the majority vote of its k nearest neighbors in the training set. The k -NN accuracy is computed as the proportion of correctly classified test samples. This evaluation provides insights into whether θ_u preserves meaningful, transferable feature embeddings that are effective for downstream tasks.

A.3. Downstream Datasets.

For our evaluation framework, we employ three diverse downstream datasets: *Office-Home* [34]: A domain adaptation benchmark comprising distinct domains, we use: Real World, Art, Clipart, and Product. It includes 65 classes with over 15,500 images, providing a robust basis for cross-domain transfer learning. *CUB-200-2011*(CUB) [35]: The Caltech-UCSD Birds dataset features fine-grained classification with 200 bird species and 11,788 images, suitable for evaluating detailed representational quality. *DomainNet-126* [30]: A multi-source domain dataset containing several domains, we use: Clipart, Painting, Real, and Sketch. This dataset includes 126 classes, offering a challenging environment for domain generalization tasks.

B. Implementation Details

B.1. Training and Retraining Details

For the experiments, both the original and retrained models are required. In the case of ResNet-50, we trained the model from scratch. For ConvNeXt-T and Swin-T, we initialized

them with ImageNet-21K pretrained weights [19]. Detailed configuration information is provided in Table 2.

Table 2. Training Details for Original and Retrain Models.

Settings	ImageNet-1K		
	ResNet-50	ConvNeXt-T	Swin-T
Epochs	182	30	30
Batch Size		256	
Learning Rate		0.1	
Optimizer	SGD	AdamW	
Momentum		0.9	
Scheduler	Step	CosineAnnealing	

B.2. Unlearning Details

We refer to the hyperparameters from the original studies. However, because most prior works proposed and tested these methods primarily on smaller datasets (e.g., CIFAR-10, CIFAR-100), critical implementation details are not fully specified when removing multiple classes from large-scale datasets. To address this limitation, we perform a grid search for each method to identify the optimal learning rate and number of epochs. Specifically, we retrain the model (excluding the forget set \mathcal{D}_f) using the same learning rate and epochs as in the original training for the Retrain method. We limit FT at 40 epochs to mitigate excessive time costs. For PL, GA, RL, and SalUn, we find that strong unlearning can be achieved within 10 epochs on large-scale data. Finally, considering the balance of logit-based and representation-based metrics, we fix the maximum epochs for DUCK, CU, SCAR, and SCRUB at 15, 80, 20, and 90, respectively. These upper limits are determined first under the scenario of Random 100 class unlearning. For Random k class experiments ($k \in \{100, 200, 300\}$), we choose the actual number of epochs while respecting these maximum values, guided by the H-LR score. For Top k class unlearning, we reuse the hyperparameter configurations established in the corresponding Random k setting.

C. Additional Experiments

We also provide t-SNE visualization of all models in Fig. 10. Our full results in all unlearning baselines across all unlearning scenarios can be found in Tables 4, 5, 6, and 7.

C.1. CKA Similarities between the Original Model and the Retrained Model.

We analyze the CKA similarities between θ_o and θ_r under different unlearning scenarios in Fig. 11. As expected, CKA similarities decrease under top class-wise forgetting scenarios and with increasing numbers of forgetting classes.

Table 3. Unlearning evaluation with 100 random class-wise forgetting on ConNeXt and Swin Transformers.

Backbone	Method	ImageNet-1K					Office-Home, CUB, DomainNet-126				
		FA	RA	TFA	TRA	Avg. Gap	AGL \uparrow	Avg. k -NN Gap	Avg. CKA	AGR \uparrow	H-LR \uparrow
ConvNeXt-T	Retrained	0.0 (0.0)	92.7 (0.0)	0.0 (0.0)	81.0 (0.0)	0.0	1.00	0.0	100.0	1.00	1.00
	FT	79.4 (79.4)	92.5 (0.2)	65.7 (65.7)	80.7 (0.3)	36.4	0.07	4.2	86.0	0.88	0.13
	GA	0.6 (0.6)	0.8 (91.9)	0.6 (0.6)	0.8 (71.2)	41.1	0.02	31.1	34.7	0.19	0.03
	RL	0.5 (0.5)	0.7 (92.0)	0.4 (0.4)	0.6 (80.4)	43.3	0.02	37.7	28.8	0.12	0.03
	PL	1.5 (1.5)	89.9 (2.8)	1.0 (1.0)	79.8 (0.9)	1.6	0.94	3.4	83.9	0.85	0.89
	SalUn	0.5 (0.5)	0.7 (92.0)	0.5 (0.5)	0.6 (80.4)	43.4	0.02	38.1	30.1	0.12	0.03
	CU	2.8 (2.8)	83.4 (6.6)	3.0 (3.0)	78.0 (3.0)	3.9	0.83	3.0	81.2	0.81	0.82
	SCRUB	0.0 (0.0)	0.1 (92.6)	0.0 (0.0)	0.1 (80.9)	43.4	0.01	47.3	17.4	0.05	0.02
Swin-T	Retrained	0.0 (0.0)	90.0 (0.0)	0.0 (0.0)	81.2 (0.0)	0.0	1.00	0.0	100.0	1.00	1.00
	FT	63.4 (63.4)	88.6 (1.4)	55.8 (55.8)	81.3 (0.1)	30.2	0.16	2.6	89.6	0.89	0.27
	GA	0.0 (0.0)	0.1 (89.9)	0.0 (0.0)	0.0 (81.2)	42.8	0.02	32.1	35.4	0.20	0.03
	RL	6.4 (6.4)	8.0 (80.6)	6.3 (6.3)	7.4 (73.8)	41.8	0.05	24.3	54.5	0.38	0.09
	PL	4.3 (4.3)	86.2 (3.8)	3.1 (3.1)	80.2 (1.0)	3.1	0.88	4.1	88.4	0.86	0.87
	SalUn	6.4 (6.4)	8.0 (80.6)	6.5 (6.5)	7.7 (73.5)	41.8	0.05	24.1	54.5	0.38	0.09
	CU	2.1 (2.1)	80.0 (10.0)	2.2 (2.2)	77.0 (4.3)	4.7	0.82	2.9	84.3	0.84	0.83
	SCRUB	8.2 (8.2)	28.0 (52.0)	8.8 (8.8)	31.8 (49.2)	29.6	0.20	14.8	56.6	0.49	0.29

C.2. Backbone Architectures.

Table 3 provides an extended comparison of the baselines using alternative backbones, specifically ConvNeXt-T [25] and Swin-T [24]. We only compare model-agnostic methods.

Table 4. Comparison of logit-based evaluation across different unlearning baselines. Each block (Random, Office-Home Top, CUB Top, DomainNet-126 Top) indicates the subset of classes removed. For each subset, we report Accuracy on ImageNet-1k.

# Unlearned classes	Method	Random					Office-Home Top					CUB Top					DomainNet-126 Top				
		FA	RA	TFA	TRA	Avg. Gap	FA	RA	TFA	TRA	Avg. Gap	FA	RA	TFA	TRA	Avg. Gap	FA	RA	TFA	TRA	Avg. Gap
100	Retrained	0.0 (0.0)	76.0 (0.0)	0.0 (0.0)	75.6 (0.0)	0.0	0.0 (0.0)	76.2 (0.0)	0.0 (0.0)	76.1 (0.0)	0.0	0.0 (0.0)	74.9 (0.0)	0.0 (0.0)	74.3 (0.0)	0.0	0.0 (0.0)	76.4 (0.0)	0.0 (0.0)	75.9 (0.0)	0.0
	FT	9.9 (9.9)	79.5 (3.5)	10.5 (10.5)	76.0 (0.4)	6.1	7.1 (7.1)	80.1 (4.1)	6.6 (6.6)	77.2 (1.1)	4.7	24.4 (24.4)	78.5 (3.6)	28.4 (28.4)	74.9 (0.6)	14.3	10.8 (10.8)	79.6 (3.2)	11.7 (11.7)	76.3 (0.4)	6.5
	GA	1.5 (1.5)	11.4 (64.6)	1.5 (1.5)	11.3 (64.3)	33.0	0.5 (0.5)	0.2 (76.0)	0.4 (0.4)	0.2 (75.9)	38.2	0.1 (0.1)	3.6 (71.3)	0.0 (0.0)	3.8 (70.5)	35.5	0.0 (0.0)	0.4 (76.0)	0.0 (0.0)	0.5 (75.4)	37.7
	RL	6.3 (6.3)	14.3 (61.7)	5.5 (5.5)	13.0 (62.6)	34.3	0.3 (0.3)	4.5 (71.7)	0.1 (0.1)	3.6 (72.5)	36.6	9.6 (9.6)	40.2 (34.7)	6.4 (6.4)	34.7 (39.6)	22.4	7.3 (7.3)	18.2 (58.2)	6.2 (6.2)	16.6 (59.3)	32.7
	PL	1.0 (1.0)	79.5 (3.5)	1.0 (1.0)	76.9 (0.9)	1.6	1.1 (1.1)	80.0 (3.8)	1.0 (1.0)	77.9 (1.8)	2.0	0.7 (0.7)	78.6 (3.7)	0.6 (0.6)	75.5 (1.2)	1.6	1.1 (1.1)	79.5 (3.1)	1.0 (1.0)	77.0 (1.1)	1.6
	SalUn	10.4 (10.4)	22.1 (53.9)	9.3 (9.3)	19.1 (56.5)	32.5	1.6 (1.6)	6.4 (69.8)	1.4 (1.4)	4.9 (71.2)	36.0	5.2 (5.2)	30.3 (44.6)	3.2 (3.2)	25.8 (48.5)	25.4	7.4 (7.4)	17.3 (59.1)	6.2 (6.2)	16.5 (59.4)	33.0
	DUCK	0.9 (0.9)	74.6 (1.4)	0.9 (0.9)	74.5 (1.1)	1.1	1.5 (1.5)	73.9 (2.3)	1.4 (1.4)	74.4 (1.7)	1.7	6.8 (6.8)	74.7 (0.2)	8.5 (8.5)	73.6 (0.7)	4.1	1.7 (1.7)	76.8 (0.4)	2.1 (2.1)	76.0 (0.1)	1.1
	CU	2.1 (2.1)	73.9 (2.1)	2.2 (2.2)	73.3 (2.3)	2.2	1.3 (1.3)	59.8 (16.4)	1.5 (1.5)	61.1 (15.0)	8.6	0.5 (0.5)	43.4 (31.5)	0.4 (0.4)	46.2 (28.1)	15.1	2.0 (2.0)	73.3 (3.1)	2.9 (2.9)	73.0 (2.9)	2.7
	SCAR	4.2 (4.2)	80.5 (4.5)	3.9 (3.9)	77.4 (1.8)	3.6	5.0 (5.0)	81.3 (5.1)	5.0 (5.0)	78.7 (2.6)	4.4	29.0 (29.0)	76.1 (1.2)	33.4 (33.4)	74.6 (0.3)	16.0	13.0 (13.0)	77.1 (0.7)	13.4 (13.4)	76.0 (0.1)	6.8
	SCRUB	1.1 (1.1)	67.3 (8.7)	1.1 (1.1)	65.7 (9.9)	5.2	0.0 (0.0)	0.1 (76.1)	0.0 (0.0)	0.1 (76.0)	38.0	0.0 (0.0)	3.5 (71.4)	0.0 (0.0)	4.2 (70.1)	35.4	0.0 (0.0)	2.0 (74.4)	0.0 (0.0)	2.8 (73.1)	36.9
200	Retrained	0.0 (0.0)	77.7 (0.0)	0.0 (0.0)	77.0 (0.0)	0.0	0.0 (0.0)	78.6 (0.0)	0.0 (0.0)	78.2 (0.0)	0.0	0.0 (0.0)	75.4 (0.0)	0.0 (0.0)	74.2 (0.0)	0.0	0.0 (0.0)	78.5 (0.0)	0.0 (0.0)	77.7 (0.0)	0.0
	FT	11.7 (11.7)	80.7 (3.0)	13.0 (13.0)	77.2 (0.2)	7.0	21.1 (21.1)	84.4 (5.8)	20.1 (20.1)	67.1 (11.1)	14.5	44.5 (44.5)	82.0 (6.6)	46.9 (46.9)	77.0 (2.8)	25.2	17.3 (17.3)	84.1 (5.6)	17.9 (17.9)	80.4 (2.7)	10.9
	GA	0.1 (0.1)	0.3 (77.4)	0.1 (0.1)	0.2 (76.8)	38.6	0.2 (0.2)	0.6 (78.0)	0.2 (0.2)	0.5 (77.7)	39.0	0.1 (0.1)	3.6 (71.8)	0.1 (0.1)	3.2 (71.0)	35.8	0.3 (0.3)	0.5 (78.0)	0.2 (0.2)	0.7 (77.0)	38.9
	RL	4.4 (4.4)	8.0 (69.7)	3.8 (3.8)	6.4 (70.6)	37.1	15.7 (15.7)	33.9 (44.7)	14.6 (14.6)	31.9 (46.3)	30.3	17.1 (17.1)	42.1 (33.3)	13.2 (13.2)	36.2 (38.0)	25.4	19.1 (19.1)	29.5 (48.7)	17.9 (17.9)	27.8 (49.9)	33.9
	PL	1.2 (1.2)	80.2 (2.5)	1.0 (1.0)	78.1 (1.1)	1.5	1.1 (1.1)	81.1 (2.5)	1.0 (1.0)	79.5 (1.3)	1.5	0.9 (0.9)	78.2 (2.8)	0.9 (0.9)	75.4 (1.2)	1.5	1.2 (1.2)	80.6 (2.1)	1.0 (1.0)	78.9 (1.2)	1.4
	SalUn	9.7 (9.7)	14.4 (63.3)	8.5 (8.5)	12.6 (64.4)	36.5	7.9 (7.9)	18.3 (60.3)	7.3 (7.3)	16.8 (61.4)	34.2	3.3 (3.3)	14.7 (60.7)	2.5 (2.5)	12.2 (62.0)	32.1	9.5 (9.5)	14.0 (64.5)	9.1 (9.1)	12.8 (64.9)	37.0
	DUCK	0.8 (0.8)	78.1 (0.4)	0.8 (0.8)	77.3 (0.3)	0.6	1.0 (1.0)	78.4 (0.2)	1.2 (1.2)	78.4 (0.2)	0.7	5.7 (5.7)	74.8 (0.6)	7.0 (7.0)	73.7 (0.5)	3.5	0.7 (0.7)	78.4 (0.1)	1.0 (1.0)	77.8 (0.1)	0.5
	CU	1.0 (1.0)	79.7 (2.0)	1.2 (1.2)	77.4 (0.4)	1.2	0.8 (0.8)	79.5 (0.9)	1.1 (1.1)	78.0 (0.2)	0.8	3.4 (3.4)	75.5 (0.1)	4.6 (4.6)	73.5 (0.7)	2.2	1.4 (1.4)	75.7 (2.8)	1.9 (1.9)	75.4 (2.3)	2.1
	SCAR	15.0 (15.0)	80.8 (3.1)	15.6 (15.6)	78.7 (1.7)	8.9	13.7 (13.7)	79.1 (0.5)	13.7 (13.7)	78.4 (0.2)	7.0	35.5 (35.5)	75.9 (0.5)	37.1 (37.1)	74.4 (0.2)	18.3	11.3 (11.3)	78.8 (0.3)	12.5 (12.5)	78.1 (0.4)	6.1
	SCRUB	18.3 (18.3)	72.5 (2.2)	16.9 (16.9)	69.7 (7.3)	11.9	0.0 (0.0)	0.1 (78.5)	0.0 (0.0)	0.1 (78.1)	39.2	0.0 (0.0)	3.9 (71.5)	0.0 (0.0)	5.0 (69.2)	35.2	0.2 (0.2)	1.2 (77.3)	0.3 (0.3)	1.8 (75.9)	38.4
300	Retrained	0.0 (0.0)	78.9 (0.0)	0.0 (0.0)	77.6 (0.0)	0.0	0.0 (0.0)	80.7 (0.0)	0.0 (0.0)	79.9 (0.0)	0.0	0.0 (0.0)	76.9 (0.0)	0.0 (0.0)	75.1 (0.0)	0.0	0.0 (0.0)	80.3 (0.0)	0.0 (0.0)	79.7 (0.0)	0.0
	FT	14.0 (14.0)	82.0 (3.1)	15.4 (15.4)	78.9 (1.3)	8.5	28.4 (28.4)	85.3 (4.6)	28.6 (28.6)	82.3 (2.4)	16.0	45.5 (45.5)	82.7 (5.8)	46.7 (46.7)	77.7 (2.6)	25.2	21.7 (21.7)	85.4 (5.1)	22.3 (22.3)	82.3 (2.6)	12.9
	GA	0.3 (0.3)	0.3 (78.6)	0.2 (0.2)	0.3 (77.3)	39.1	0.2 (0.2)	0.2 (80.5)	0.2 (0.2)	0.3 (79.6)	40.1	0.2 (0.2)	2.0 (74.9)	0.2 (0.2)	1.8 (73.3)	37.2	0.2 (0.2)	0.3 (80.0)	0.2 (0.2)	0.4 (79.3)	39.9
	RL	6.4 (6.4)	9.0 (69.9)	5.5 (5.5)	8.1 (69.5)	37.8	11.5 (11.5)	22.9 (57.8)	10.2 (10.2)	21.2 (58.7)	34.6	11.9 (11.9)	24.1 (52.7)	9.2 (9.2)	20.7 (54.4)	32.0	14.4 (14.4)	19.4 (60.9)	13.3 (13.3)	18.0 (61.7)	37.6
	PL	1.0 (1.0)	81.1 (2.2)	0.9 (0.9)	79.3 (1.7)	1.5	1.0 (1.0)	81.9 (1.2)	1.0 (1.0)	81.0 (1.0)	1.1	1.0 (1.0)	78.6 (1.7)	0.9 (0.9)	76.0 (0.9)	1.1	1.0 (1.0)	81.9 (1.6)	0.8 (0.8)	80.9 (1.2)	1.2
	SalUn	10.5 (10.5)	14.3 (64.6)	8.6 (8.6)	12.4 (65.2)	37.2	8.3 (8.3)	14.7 (66.0)	8.2 (8.2)	13.4 (66.5)	37.3	7.3 (7.3)	17.0 (59.9)	6.0 (6.0)	15.3 (59.8)	33.3	10.5 (10.5)	14.5 (65.8)	9.5 (9.5)	13.4 (66.3)	38.0
	DUCK	0.9 (0.9)	79.5 (0.6)	1.0 (1.0)	75.6 (2.0)	1.1	2.4 (2.4)	80.2 (0.5)	2.7 (2.7)	80.0 (0.1)	1.4	9.3 (9.3)	76.5 (0.4)	11.5 (11.5)	74.6 (0.5)	5.4	1.7 (1.7)	80.4 (0.1)	1.9 (1.9)	80.3 (0.6)	1.1
	CU	0.7 (0.7)	81.1 (2.2)	0.8 (0.8)	78.6 (1.0)	1.2	1.6 (1.6)	81.5 (0.8)	2.0 (2.0)	79.9 (0.0)	1.1	6.7 (6.7)	77.9 (1.0)	8.8 (8.8)	74.9 (0.2)	4.2	1.0 (1.0)	82.0 (1.7)	1.2 (1.2)	80.7 (1.0)	1.2
	SCAR	13.7 (13.7)	81.7 (2.8)	14.6 (14.6)	80.0 (2.4)	8.4	20.8 (20.8)	82.7 (1.2)	21.0 (21.0)	81.7 (1.8)	11.4	40.5 (40.5)	79.6 (2.7)	41.1 (41.1)	76.9 (1.8)	21.4	15.1 (15.1)	82.7 (2.4)	15.6 (15.6)	81.8 (2.1)	8.8
	SCRUB	55.6 (55.6)	80.9 (2.0)	51.7 (51.7)	77.5 (0.1)	27.4	0.1 (0.1)	0.1 (80.6)	0.1 (0.1)	0.1 (79.8)	40.2	0.2 (0.2)	3.9 (73.0)	0.2 (0.2)	4.5 (70.6)	36.0	1.1 (1.1)	12.9 (67.4)	1.1 (1.1)	15.6 (64.1)	33.4

Table 5. Comparison of k -NN performance across different unlearning subsets. Each block (Random, Office-Home Top, CUB Top, DomainNet-126 Top) indicates the subset of classes removed. For each subset, we report k -NN Accuracy on three downstream tasks (Office-Home, CUB, and DomainNet-126) to gauge transferability.

# Unlearned classes	Method	Random			Office-Home Top	CUB Top	DomainNet-126 Top
		Office-Home k -NN	CUB k -NN	DomainNet-126 k -NN	Office-Home k -NN	CUB k -NN	DomainNet-126 k -NN
100	Original	80.3 (3.0)	43.4 (6.5)	84.0 (2.0)	80.3 (14.2)	43.4 (19.5)	84.0 (3.4)
	Retrained	77.3 (0.0)	36.9 (0.0)	82.0 (0.0)	66.1 (0.0)	23.9 (0.0)	80.6 (0.0)
	FT	78.4 (1.1)	39.0 (2.1)	81.6 (0.4)	73.1 (7.0)	34.5 (10.6)	81.0 (0.4)
	GA	29.7 (47.6)	10.4 (26.5)	42.2 (39.8)	12.7 (53.4)	3.0 (20.9)	20.5 (60.1)
	RL	44.0 (33.3)	8.0 (28.9)	35.2 (46.8)	47.8 (34.2)	4.6 (19.3)	40.5 (40.1)
	PL	80.3 (3.0)	43.3 (6.4)	84.0 (2.0)	76.2 (10.1)	37.3 (13.4)	83.3 (2.7)
	SalUn	38.5 (38.8)	8.0 (28.9)	42.5 (39.5)	25.5 (40.6)	3.7 (20.2)	40.5 (40.1)
	DUCK	79.8 (2.5)	39.0 (2.1)	82.7 (0.7)	73.6 (7.5)	33.6 (9.7)	82.3 (1.7)
	CU	75.8 (1.5)	33.9 (3.0)	80.1 (1.9)	53.3 (12.8)	13.7 (9.2)	77.6 (3.0)
	SCAR	78.0 (0.7)	42.8 (5.9)	83.1 (1.1)	78.1 (12.0)	38.5 (14.6)	82.9 (2.3)
SCRUB	74.7 (2.6)	42.2 (5.3)	80.9 (1.1)	8.9 (57.2)	5.3 (18.6)	40.8 (39.8)	
200	Retrained	77.9 (0.0)	34.9 (0.0)	81.2 (0.0)	63.3 (0.0)	19.1 (0.0)	78.2 (0.0)
	FT	77.0 (0.9)	37.2 (2.3)	81.7 (0.5)	77.9 (14.6)	16.3 (2.8)	84.0 (5.8)
	GA	13.0 (64.9)	2.4 (32.5)	20.0 (61.2)	14.7 (48.6)	3.3 (15.8)	19.6 (58.6)
	RL	40.5 (37.4)	8.7 (26.2)	52.9 (28.3)	31.1 (32.2)	5.4 (13.7)	46.9 (31.3)
	PL	79.4 (1.5)	41.4 (6.5)	83.7 (2.5)	76.4 (13.1)	36.0 (16.9)	83.4 (5.2)
	SalUn	28.8 (49.1)	5.7 (29.2)	36.5 (44.7)	23.6 (39.7)	4.7 (14.4)	37.8 (40.4)
	DUCK	78.0 (0.1)	39.6 (4.7)	70.6 (10.6)	71.9 (8.6)	29.5 (10.4)	81.8 (3.6)
	CU	80.2 (2.3)	43.6 (8.7)	83.2 (2.1)	72.7 (9.4)	28.2 (9.1)	77.1 (1.1)
	SCAR	80.7 (2.8)	41.6 (6.7)	84.0 (2.8)	75.3 (12.0)	38.5 (19.4)	83.2 (5.0)
SCRUB	78.1 (0.2)	34.0 (0.9)	80.7 (0.5)	13.8 (49.5)	5.6 (13.5)	31.7 (46.5)	
300	Retrained	75.5 (0.0)	30.3 (0.0)	79.8 (0.0)	55.1 (0.0)	14.0 (0.0)	77.1 (0.0)
	FT	77.8 (2.3)	38.0 (7.7)	81.8 (2.0)	78.0 (22.9)	35.8 (21.8)	83.8 (6.7)
	GA	15.9 (59.6)	2.6 (27.7)	17.8 (62.0)	12.7 (42.4)	2.7 (11.3)	17.4 (59.7)
	RL	31.1 (44.4)	6.6 (23.7)	37.8 (42.0)	27.0 (28.1)	6.3 (7.7)	41.3 (35.8)
	PL	80.1 (4.6)	38.7 (8.4)	83.8 (4.0)	75.6 (20.5)	35.8 (21.8)	83.2 (6.1)
	SalUn	30.6 (44.9)	7.0 (23.3)	37.8 (42.0)	22.0 (33.1)	6.8 (7.2)	38.2 (38.9)
	DUCK	79.4 (3.9)	40.2 (9.9)	82.5 (2.7)	71.3 (16.2)	32.7 (18.7)	82.2 (5.1)
	CU	77.5 (2.0)	40.0 (9.7)	82.9 (3.1)	70.6 (15.5)	29.9 (15.9)	82.5 (5.4)
	SCAR	80.5 (5.0)	42.4 (12.1)	83.6 (3.8)	77.3 (22.2)	37.5 (23.5)	83.7 (6.6)
SCRUB	78.7 (3.2)	39.4 (9.1)	82.9 (3.1)	13.8 (41.3)	5.6 (8.4)	65.4 (11.7)	

Table 6. Comparison of CKA values between θ_u and θ_r across different unlearning subsets. Each block (Random, Office-Home Top, CUB Top, DomainNet-126 Top) indicates the subset of classes removed. For each subset, we report CKA value on three downstream tasks (Office-Home, CUB, and DomainNet-126) to gauge representation quality.

Unlearned classes	Method	Random				Office-Home Top	CUB Top	DomainNet-126 Top
		Office-Home CKA	CUB CKA	DomainNet-126 CKA	Avg. CKA	Office-Home CKA	CUB CKA	DomainNet-126 CKA
100	Original	89.8 (10.2)	82.1 (17.9)	81.8 (18.2)	84.6	83.0 (17.0)	69.7 (30.3)	80.4 (19.6)
	Retrained	100.0 (0.0)	100.0 (0.0)	100.0 (0.0)	100.0	100.0 (0.0)	100.0 (0.0)	100.0 (0.0)
	FT	87.6 (12.4)	79.0 (21.0)	79.9 (20.1)	82.2	82.4 (17.6)	66.9 (33.1)	78.9 (21.1)
	GA	8.3 (91.7)	9.8 (90.2)	10.2 (89.8)	9.4	17.5 (82.5)	20.1 (79.9)	20.0 (80.0)
	RL	6.3 (93.7)	5.8 (94.2)	4.7 (95.3)	5.6	24.4 (75.6)	17.8 (82.2)	12.3 (87.7)
	PL	91.6 (8.4)	84.7 (15.3)	84.5 (15.5)	86.9	87.3 (12.7)	75.0 (25.0)	83.5 (16.5)
	SalUn	9.7 (90.3)	8.0 (92.0)	8.5 (91.5)	8.7	11.6 (88.4)	24.9 (75.1)	12.4 (87.6)
	DUCK	90.7 (9.3)	83.2 (16.8)	84.9 (15.1)	86.3	88.2 (11.8)	78.2 (21.8)	87.7 (12.3)
	CU	85.6 (14.4)	75.9 (24.1)	76.1 (23.9)	79.2	10.1 (89.9)	5.2 (94.8)	72.2 (27.8)
	SCAR	74.2 (25.8)	65.4 (34.6)	58.8 (41.2)	66.1	69.0 (31.0)	74.0 (26.0)	83.6 (16.4)
SCRUB	68.9 (31.1)	63.8 (36.2)	52.8 (47.2)	61.8	5.7 (94.3)	33.1 (66.9)	29.3 (70.7)	
200	Original	88.6 (11.4)	80.5 (19.5)	80.9 (19.1)	83.3	79.7 (20.3)	63.4 (36.6)	78.9 (21.1)
	Retrained	100.0 (0.0)	100.0 (0.0)	100.0 (0.0)	100.0	100.0 (0.0)	100.0 (0.0)	100.0 (0.0)
	FT	87.0 (13.0)	77.6 (22.4)	78.9 (21.1)	81.2	82.4 (17.6)	70.7 (29.3)	82.8 (17.2)
	GA	13.2 (86.8)	9.8 (90.2)	17.3 (82.7)	13.4	16.9 (83.1)	24.6 (75.4)	19.6 (80.4)
	RL	12.9 (87.1)	10.7 (89.3)	12.9 (87.1)	12.2	25.8 (74.2)	22.6 (77.4)	12.4 (87.6)
	PL	91.3 (8.7)	83.1 (16.9)	84.6 (15.4)	86.3	83.7 (16.3)	70.1 (29.9)	82.7 (17.3)
	SalUn	9.8 (90.2)	6.3 (93.7)	11.7 (88.3)	9.3	12.7 (87.3)	5.5 (94.5)	9.8 (90.2)
	DUCK	92.4 (7.6)	84.5 (15.5)	87.7 (12.3)	88.2	85.8 (14.2)	74.5 (25.5)	86.7 (13.3)
	CU	91.3 (8.7)	83.9 (16.1)	84.7 (15.3)	86.6	84.6 (15.4)	63.9 (36.1)	74.0 (26.0)
	SCAR	91.1 (8.9)	83.1 (16.9)	85.0 (15.0)	86.4	83.3 (16.7)	70.6 (29.4)	82.7 (17.3)
SCRUB	75.9 (24.1)	69.6 (30.4)	48.3 (51.7)	64.6	15.9 (84.1)	41.5 (58.5)	18.6 (81.4)	
300	Original	86.8 (13.2)	76.8 (23.2)	80.2 (19.8)	81.3	76.7 (23.3)	59.6 (40.4)	77.3 (22.7)
	Retrained	100.0 (0.0)	100.0 (0.0)	100.0 (0.0)	100.0	100.0 (0.0)	100.0 (0.0)	100.0 (0.0)
	FT	86.3 (13.7)	73.4 (26.6)	78.1 (21.9)	79.3	79.7 (20.3)	67.5 (32.5)	80.5 (19.5)
	GA	12.8 (87.2)	10.5 (89.5)	10.7 (89.3)	11.3	16.1 (83.9)	23.6 (76.4)	21.0 (79.0)
	RL	6.8 (93.2)	6.4 (93.6)	4.6 (95.4)	5.9	13.2 (86.8)	12.5 (87.5)	13.2 (86.8)
	PL	90.5 (9.5)	81.1 (18.9)	83.6 (16.4)	85.1	81.6 (18.4)	66.8 (33.2)	81.2 (18.8)
	SalUn	9.5 (90.5)	6.3 (93.7)	12.0 (88.0)	9.3	13.4 (86.6)	5.3 (94.7)	13.3 (86.7)
	DUCK	91.7 (8.3)	82.0 (18.0)	87.3 (12.7)	87.0	83.5 (16.5)	72.2 (27.8)	85.3 (14.7)
	CU	90.5 (9.5)	80.2 (19.8)	84.1 (15.9)	84.9	82.4 (17.6)	72.5 (27.5)	81.8 (18.2)
	SCAR	89.6 (10.4)	79.2 (20.8)	84.5 (15.5)	84.4	80.2 (19.8)	65.5 (34.5)	82.0 (18.0)
SCRUB	86.6 (13.4)	76.6 (23.4)	78.9 (21.1)	80.7	24.6 (75.4)	43.2 (56.8)	33.5 (66.5)	

Table 7. Comparison of the proposed metrics across different unlearning subsets. Each block (Random, Office-Home Top, CUB Top, DomainNet-126 Top) indicates the subset of classes removed. The evaluated metrics include AGL, AGR, and the unified metric H-LR. Higher AGL, AGR, and H-LR scores indicate better preservation of feature representations and overall unlearning effectiveness.

# Unlearned classes	Method	Random			Office-Home Top			CUB Top			DomainNet-126 Top		
		AGL	AGR	H-LR	AGL	AGR	H-LR	AGL	AGR	H-LR	AGL	AGR	H-LR
100	Retrained	1.00	1.00	1.00	1.00	1.00	1.00	1.00	1.00	1.00	1.00	1.00	1.00
	FT	0.78	0.81	0.79	0.82	0.77	0.79	0.52	0.60	0.56	0.76	0.79	0.77
	GA	0.12	0.06	0.08	0.06	0.08	0.07	0.08	0.16	0.11	0.06	0.08	0.07
	RL	0.12	0.04	0.06	0.08	0.16	0.11	0.33	0.14	0.20	0.15	0.07	0.10
	PL	0.94	0.84	0.89	0.92	0.78	0.84	0.94	0.65	0.77	0.94	0.81	0.87
	SalUn	0.15	0.06	0.09	0.08	0.07	0.07	0.26	0.20	0.23	0.14	0.07	0.09
	DUCK	0.96	0.85	0.90	0.93	0.82	0.87	0.85	0.71	0.77	0.96	0.86	0.91
	CU	0.92	0.78	0.84	0.69	0.09	0.16	0.49	0.05	0.09	0.90	0.70	0.79
	SCAR	0.87	0.94	0.74	0.83	0.61	0.70	0.47	0.63	0.54	0.75	0.82	0.78
	SCRUB	0.80	0.60	0.69	0.06	0.02	0.03	0.09	0.27	0.14	0.07	0.18	0.10

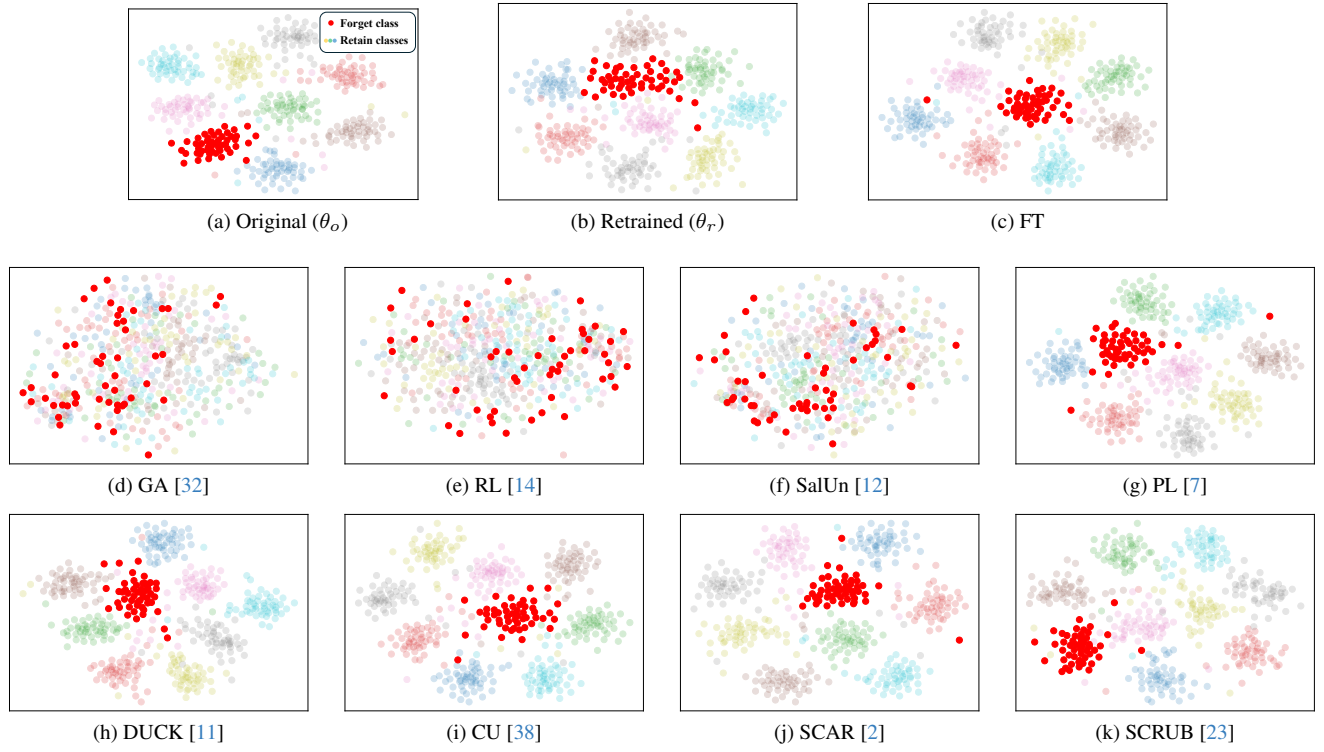


Figure 10. Visualizations of the feature representations from the original (θ_o), retrained (θ_r), and unlearned models (θ_u) on a subset of ImageNet-1K, using ResNet-50.

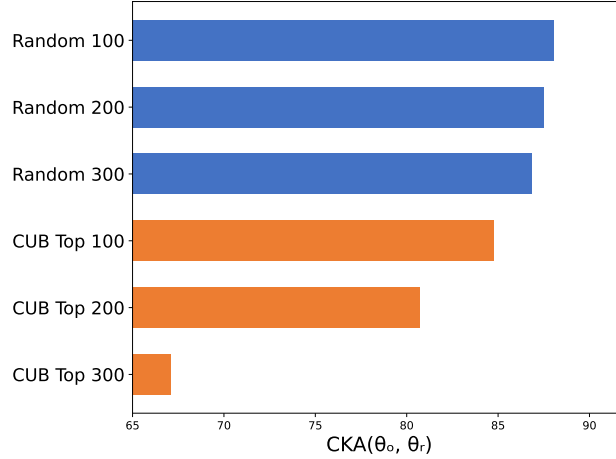


Figure 11. CKA similarities between θ_o and θ_r . The similarities decrease under top class-wise forgetting scenarios compared to random class-wise forgetting and with increasing numbers of forgetting classes.

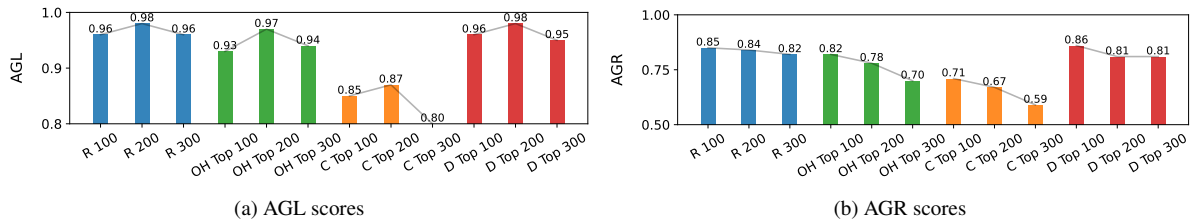


Figure 12. AGL and AGR scores in Random and Top class-wise forgetting scenarios on DUCK. (a) AGL score archives consistently high in all settings. (b) AGR scores decrease, as the number of forgetting classes increases. This is more evident in top class-wise forgetting, where θ_r has a low similarity to θ_o .